Training Course

Climate Change and its Impact on Water Resources

[May 17 - 21, 2010]

LECTURE - 10

IMPACT OF CLIMATE CHANGE ON HYDROLOGIC EXTREMES

By

RAKESH KUMAR R.P. PANDEY

Organised by

National Institute of Hydrology Roorkee- 247 667

&

Indian Institute of Technology Roorkee -247 667

IMPACT OF CLIMATE CHANGE ON HYDROLOGIC EXTREMES

INTRODUCTION

The climate varies naturally on all time-scales. Variations may occur due to forces such as volcanic eruptions or changes in the Sun's output of energy. They may also be generated by interactions among the different components of the global climate system: the atmosphere, oceans, biosphere, ice cover, and land surface. These internal interactions may cause fairly regular fluctuations, such as the El Niño phenomenon, or apparently random changes in climate.

Since the human settlements and the economical activities on the earth are largely concentrated in mid-latitudinal regions, the impacts of floods and droughts are more apparent in these regions (Ponce, 1995a; Karl, 1983). Natural variability often produces climate extremes and disasters. On time-scales of days, months, and years, variability in weather and climate can produce heat waves, frosts, flooding, droughts, severe storms, and other extremes. An important question which scientists are trying to answer is whether mankind's interference with the climate system through the enhancement of the natural greenhouse effect will increase the frequency or magnitude of extreme weather events. Given the large natural variability and the obvious rarity of extreme weather events it is hard to ascribe the observed phenomena to the enhanced greenhouse effect or even discern a definite trend in extreme event throughout this century. What can be said with certainty, however, is that any change in climate will affect society mainly through extreme weather events.

Global climate change is one of the key factors that affects the hydrological cycle. Any change in temperature affects the atmospheric moisture, precipitation and circulation pattern of the atmosphere, e.g., changes in the rate of evaporation affects the hydrological cycle. Higher temperatures turn some part of snowfall into rainfall; the snowmelt season occurs earlier, consequently the timing and volume of spring flood changes substantially (IPCC, 2001). Inconsistency of elements characterizing the processes of hydrologic cycle is responsible for occurrence of hydrologic extremes (Ponce et al. 2000) Here, the hydrologic extremes refer to the circumstances when there is either too much of water that may cause damages (floods), or too less of water that may cause water scarcity in sustaining usual regional activities and the ecosystem (droughts). Regions with higher variability of rainfall and runoff are more vulnerable to floods and droughts (Kundzewicz and Kaczmarek 2000). Floods and drought have always been a major

concern of the society. Despite fascinating achievements of science and technology in 20th century, extreme hydrological events continue to hit human heritage and undermine development by breaking continuity. Devastating droughts and floods can be viewed as enemies of sustainable development (Kundzewicz and Kaczmarek 2000). They cause damage to crops and agricultural farms and induce the threats of adversity and famine.

The primary purpose of authoring of this article is to present current level comprehension on relevance of climate change with floods and droughts in different climatic regions. It is hoped that such articles may enhance understanding and ability to cope with adverse impacts of floods and droughts on the society.

Definition of Climatic Extremes

Some definitions of climatic extremes choose to separate the nature of the event from its social and economic consequences. A climate extreme, then, is a significant departure from the normal state of the climate, irrespective of its actual impact on life or any other aspect of the Earth's ecology. When a climate extreme has an adverse impact on human welfare, it becomes a climatic disaster. In some parts of the world climatic disasters occur so frequently that they may even be considered as part of the norm. It is possible that greenhouse gas-induced climate change will alter the frequency, magnitude, and character of both climate extremes and climatic disasters.

Others have defined climatic extremes or extreme weather events as sufficiently anomalous to cause substantial socio-economic damage. In this second definition, natural and social factors are interpreted together. Thus, it is a socio-economic threshold, which is, for a suitably adapted society, rarely crossed. Rare is defined as the return period of the extreme event being substantially longer than the recovery period of the damage caused. The climatic extremes may be categorized as follows:

- Droughts (due to increased evaporation and reduced precipitation);
- River floods (due to increased precipitation);
- Landslides (due to increased precipitation);
- Storms, cyclones and tornadoes (due to changing heat transport patterns and increased land-ocean temperature differential);
- Ocean and coastal surges and related flooding (due to atmospheric pressure changes and sea level rise);
- Heat spells and cold snaps.

Signals of Climate Change

The facts of observed climate change and its reported impacts on environment and the society are summarized below (IPCC 2007):

- 1. The earth has warmed by 0.74 [0.56 to 0.92]°C during last 100-years (1906–2005).
- 2. Eleven of the last twelve years (1995 -2006) rank among the 12 warmest years in the instrumental record.
- 3. Average global ocean temperature has increased to 3000 m depth and the ocean has been absorbing more than 80% of the heat added to the climate system.
- 4. More intense and longer droughts observed over wider areas since the 1970s, in the tropics and subtropics.
- 5. The frequency of heavy precipitation events has increased over most land areas.
- 6. Significantly increased rainfall has been observed in eastern parts of North and South America, northern Europe and northern and central Asia.
- 7. Average Arctic temperatures increased at almost twice the global average rate in the past 100 years.
- 8. Cold days, cold nights and frost have become less frequent, while hot days, hot nights, and heat waves have become more frequent.
- 9. Mountain glaciers and snow cover have declined on average in both hemispheres.

Other signals of adverse impacts on society and environment are as follows

- 10. 40 % of world population now faces chronic shortage of fresh water for daily needs.
- 11. Half of the world's wetlands have been lost.
- 12. Contaminated water kills around 2.2 million people every year.
- 13. Air pollution has now become major killer accounting for death of 3 million people every year.
- 14. Since 1990, 24 % of the world's forests have been destroyed. The rate of loss is 90,000 sq. km every year.
- 15. Half the world's grasslands are overgrazed.
- 16. 800 wildlife species have become extinct and 11,000 more are threatened.
- 17. Almost 75 per cent of the world's marine captures is over fished or fully utilized. In North America, 10 fish species went extinct in the 1990s.
- 18. Two-thirds of the world's farm lands suffer from soil degradation.

Climate Change and Occurrence of Extreme Events

Global climate change could well affect the frequency, magnitude and location of extreme events. Any shift in mean climate will almost inevitably result in a change in the frequency of extreme events. In general, more heat waves and fewer frosts could be expected as the mean temperature rises. All India time series of average temperature is published by India meteorological department (IMD) is shown in Fig 1.

As the average global temperature increases one would expect that the moisture content of the atmosphere to rise, due to increased rates of evaporation from the sea surface. For every 1°C sea surface temperature rise, atmospheric moisture over the oceans increases by 6-8%. Increases in atmospheric moisture may lead to increased precipitation rates in some parts of the world (causing floods and landslides), whilst decreases may be experienced in other parts (leading to droughts) due to changes in energy and moisture transport patterns in the atmosphere. In general, as more energy and moisture is put into the atmosphere, the likelihood of storms, hurricanes and tornadoes increases (Kaczmarek et al., 1997. Computer models which simulate the effects on the global climate of doubling atmospheric carbon dioxide concentrations have revealed some alarming results. A model used by the UK Meteorological Office, for example, has projected that the daily maximum rainfall in North Western Europe will increase by 40%. Consequently, a 1 in 10 year flood becomes a 1 in 3 year flood. Another model predicts that up to 89% of years will be warmer than 1997 in the UK by the 2050s, currently the third warmest year on record. Distribution of number of low, moderate, heavy and very heavy rainfall events are shown in Fig.2 (Source: Goswami et al., Science, Dec., 2006) in northwest and some parts in southern India.

The All-India monsoon rainfall does not show any trend however small pockets of increasing and decreasing trends are observed. West coast, north Andhra Pradesh and north-west India show increasing trend in seasonal rainfall while decreasing trend is observed over east Madhya Pradesh and adjoining areas, north-east India and parts of Gujarat and Kerala (-6 to -8% of normal over 100 years). Some of the significant changes in rainfall pattern observed in India are listed below:

- Frequency of intense rainfall events has been significantly increased.
- Mean annual surface air temperatures show a significant warming of about 0.5° C/100 year during the last century.

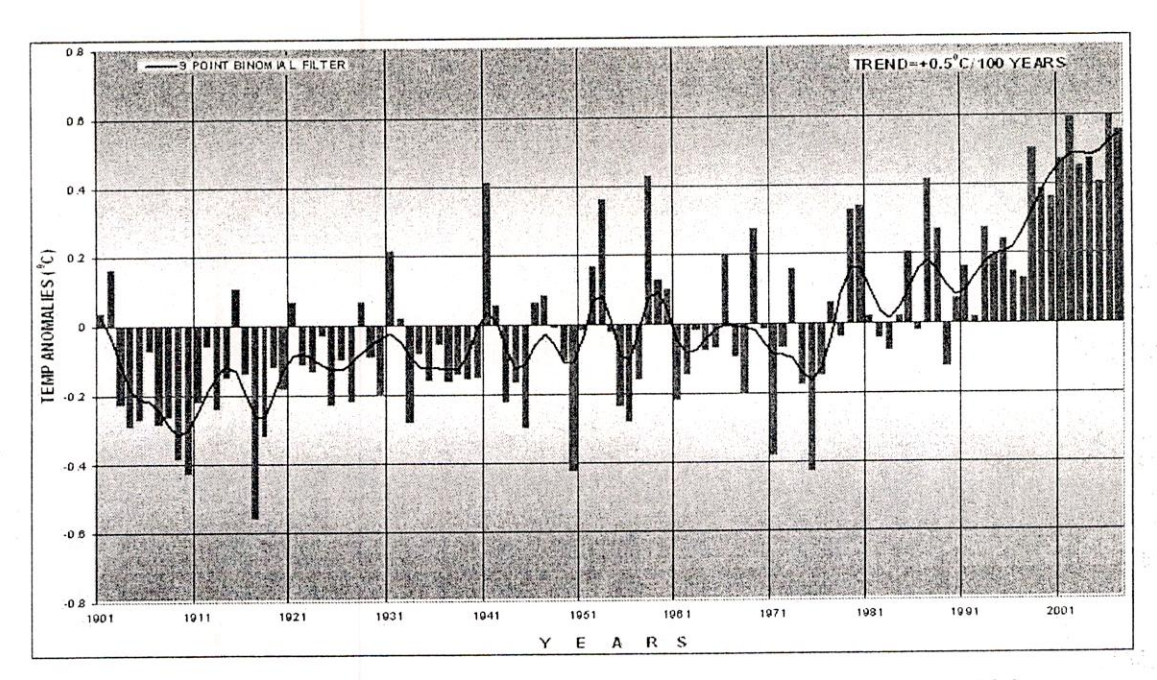


Fig.1: Time series all India of average temperature from 1901-2006

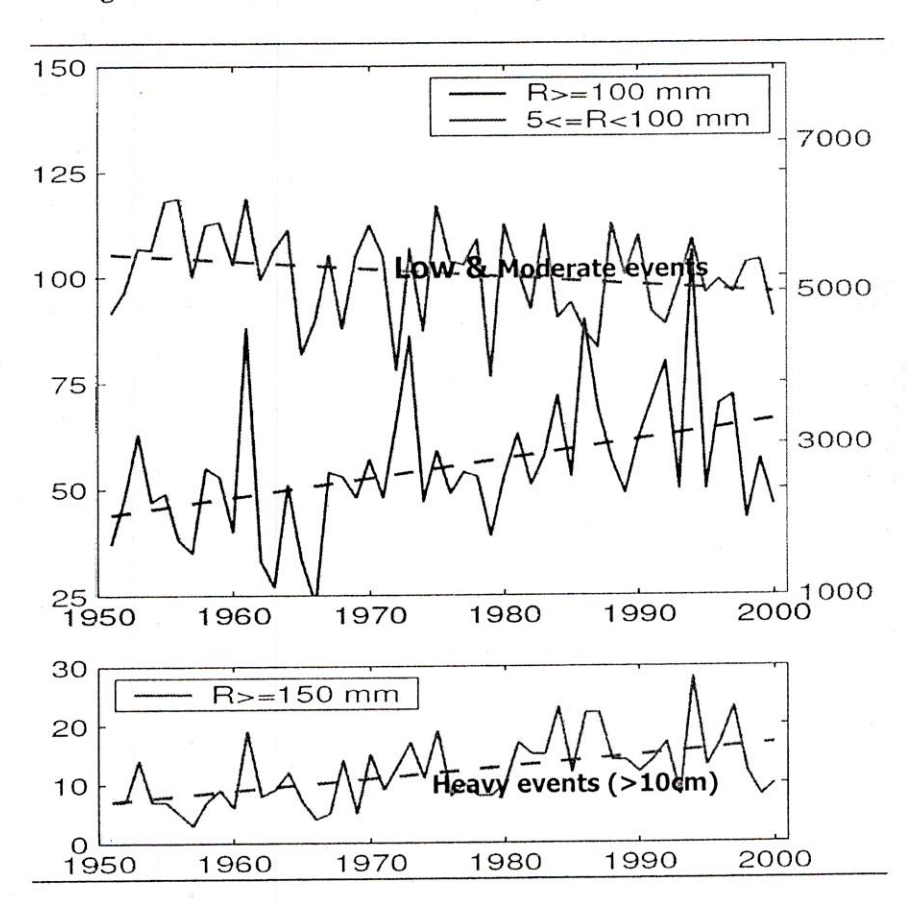


Fig. 2: Distribution of number of low, moderate and heavy rainfall events in India V. Heavy events (>15cm)

An increase in air temperature would increase potential evapo-transpiration, but the magnitude of increase also depends on changes in sunlight, humidity, wind speed, rainfall and vegetation characteristics. Actual evapo-transpiration may increase or decrease according to the availability of soil moisture. It is not certain how individual catchment areas will respond to changing evapo-transpiration rates and precipitation. It is likely, however, that drier hydrological regimes will be more sensitive to changes in climate. Relatively small changes in temperature and precipitation could cause relatively large changes in run-off. Arid and semi-arid regions will therefore be particularly sensitive to reduced rainfall and to increased evaporation and plant transpiration.

In the developed world, the return period of extreme events may still be substantially greater than the recovery period from the disasters which the events cause. For less adaptable societies in the developing world, however, a shorter *return period* of extreme events may not allow them to fully recover from the effects of one event before the next event strikes.

Evidences of Increase in Extreme Events

Every region of the world experiences record-breaking climate extremes from time to time. In 1989, for example, the "Big Wet" in eastern Australia brought torrential downpours and the worst flooding in two centuries. The same year also saw an extreme typhoon season in Southeast Asia. The Philippines was hit by three typhoons in October, including Typhoon Elsie with its peak winds of 200 km/hr. More than 1,000 people drowned a month later when southern Thailand was struck by the most powerful storm in fifty years. Many people in England will remember the "Hurricane" of October 1987. Droughts are another devastating type of climate extreme. Early this century, a trend towards increased drought in the North American Midwest culminated in the "Dust Bowl" decade of the "dirty thirties", after which conditions eased. During nine of the years since 1970, annual rainfall over the Sahel zone of northern Africa dropped more than 20% below the average prevailing during this century's first seven decades; those previous 70 years saw only one extreme of this magnitude (Wilhite Donalt, 2000). Indian subcontinent faced more frequent and severe drought events in last three decades of the last century (i.e., major drought events in 1979, 1987, 1989, 1996, 2002, and 2006) (Pandey and Ramasastri 2001, Pandey et al 2002). Major Cyclone events in India have been too frequent in last 50 years of the 20th century as can be seen in Table 1 below.

Table 1: List of major cyclone events in India

Sl.No.	Location	Date/ Area	Documented Damages
1	Bengal	Oct, 1847	75,000 people and 6000 cattle killed. Damage to property
2	Bengal	October, 1874	80,000 people killed heavy loss to property and communication disrupted.
3	Andhra Pradesh	November, 1946	750 people and 30,000 cattle lost life. Damage to property and roads also reported.
4	Tamil Nadu	December, 1972	80 people and 150 cattle killed and communication disrupted.
5	Bengal	September, 1976	10 people and 40,000 cattle lost life. Damage to property including communication
6	Andhra Pradesh	November, 1977	8547 people and 40,000 cattle lost life. Communication disrupted heavy loss to property
7	Tamil Nadu	May, 1979	700 people and 300,000 cattle lost life. Communication disrupted.
8	Orissa	September, 1985	84 people and 2600 cattle lost life. Land of 4.0 has damaged.
9	Andhra Coast	November, 1987	50 people and 25,800 cattle lost life, 84,00 houses, roads, and other communication disrupted.
10	Orissa	June, 1989	61 people and 27,000 cattle lost life, 145,000 houses, communication disrupted.
11	Andhra Pradesh	May, 1990	928 human lives lost, 14,000 houses damaged.
12	Tamil Nadu	November, 1991	185 people and 540 cattle dead. Property including roads worth 300 crores damaged.
13	Bengal	April, 1993	Over 100 causalities, communication system including road disrupted and damaged.
14	Bengal	November, 1994	More than a thousand houses damaged in 26 villages, damage to lake and fisheries, disrupted all communication.
15	Andhra Coast	October, 1996	1057 causalities, 647,000 houses damaged road network completely damaged.
16	Gujarat	June, 1998	1261 casualties, 2.57 lakh houses damaged.
17	Orissa	October, 1999	10,086 Casualties, 21.6 Lakh houses damaged.

Frequent reports of record-breaking events suggest that climate extremes are becoming more common. There are few documented scientific evidences indicating greater frequency of climatic extremes at the global level. The most recent Intergovernmental Panel on Climate Change scientific assessment (IPCC 2001) concluded that it was likely that higher maximum and minimum temperatures, more hot days and fewer cold days, and more intense precipitation events have been observed in the latter half of the 20th century. Nevertheless, it is still plausible that increased human vulnerability to climate extremes (particularly in developing countries) is transforming extreme events into climatic disasters. This is because people in many parts of the

world are being forced to live in more exposed and marginal areas. In other areas, high-value property is being developed in high-risk zones. This explains, for example, why Hurricane Hugo, which devastated the Caribbean and southern United States in 1989, proved the costliest hurricane in history, with an estimated \$10 billion in damages. Finally, because the communications revolution has made news and information more widely available than ever before, people are much more aware of the occurrence of extreme events and of their impact.

The earth has warmed by 0.74 during last 100-years (1906–2005). Noticeable changes in climatic attributes could be observes after 1981 and the last decade was warmest among all. The average global ocean temperature has increased to 3000 m depth. More intense and longer droughts have been observed over wider areas since the 1970s, in the tropics and subtropics. It is widely recognized that the frequency of severe drought events may increase significantly. Also, the frequency of heavy precipitation events and floods has increased over most land areas. However, current documented evidences still need comprehensive verification to conclude that the extreme events are the first signs of climate change. There is need to develop better understanding on the climate system and the effects of greenhouse gas emissions well enough to conclude that particular events are linked to the problem. Nevertheless, monitoring and studying extreme events, and learning how to predict and cope with them, must be a priority. Of all aspects of climate variability, extreme events are likely to have greatest effect on human wellbeing in the decades to come. What is most certain, however, is that it is likely to be the poorest and most vulnerable societies in the developing world which will be least able to adapt to any increase in the frequency and magnitude of extreme weather phenomena.

FLOOD FREQUENCY ESTIMATION AND IMPACT OF CLIMATE CHANGE

Information on flood magnitudes and their frequencies is needed for design of various types of water resources projects/ hydraulic structures such as dams, spillways, road and railway bridges, culverts, urban drainage systems as well as for taking up various non-structural measures such as flood plain zoning, economic evaluation of flood protection projects etc. Since scientific hydrology began in the seventeenth century, one of the most difficult problems facing engineers and hydrologists is how to predict flow in basins with no records. Whenever, rainfall or river flow records are not available at or near the site of interest, it is difficult for hydrologists or engineers to derive reliable design flood estimates, directly. Also, there are situations when

river flow records are available for a short period of time for a number of sites for a region. In such a situation, regional flood frequency relationships developed for the region are one of the alternative methods for prediction of design floods, especially for small to medium size catchments. Thus regional flood frequency analysis is a procedure for substitution of space for time.

Considering the importance of prediction in ungauged catchments, the International Association of Hydrological Sciences (IAHS) launched "Prediction of Ungauged Basins (PUBs)" as one of its initiatives and declared the current decade as "Decade of PUBs". As per the Indian design criteria, frequency based floods find their applications in estimation of design floods for almost all the types of hydraulic structures viz. small size dams, barrages, weirs, road and railway bridges, cross drainage structures, flood control structures etc., excluding large and intermediate size dams. For design of large and intermediate size dams probable maximum flood and standard project flood are adopted, respectively. Most of the small size catchments are ungauged or sparsely gauged. To overcome the problems of prediction of floods of various return periods for ungauged and sparsely gauged catchments, a robust procedure of regional flood frequency estimation is required to be developed.

L-moments Approach

L-moments are a recent development within statistics (Hosking, 1990). In a wide range of hydrologic applications, L-moments provide simple and reasonably efficient estimators of characteristics of hydrologic data and of a distribution's parameters (Stedinger et al., 1992). Like the ordinary product moments, L-moments summarize the characteristics or shapes of theoretical probability distributions and observed samples. Both moment types offer measures of distributional location (mean), scale (variance), skewness (shape), and kurtosis (peakedness).

Probability Weighted Moments and L-Moments

The L-moments are an alternative system of describing the shapes of probability distributions (Hosking and Wallis, 1997). They arose as modifications of probability weighted moments (PWMs) of Greenwood et al. (1979). Probability weighted moments are defined as:

$$\beta_{\mathbf{r}} = \mathbf{E} \left(\mathbf{x} \{ \mathbf{F}(\mathbf{x}) \}^{\mathbf{r}} \right) \tag{1.1}$$

which, can be rewritten as:

$$\beta_r = \int_0^1 x(\mathbf{F}) \mathbf{F}^r d\mathbf{F}$$
 (1.2)

where, F = F(x) is the cumulative distribution function (CDF) for x, x(F) is the inverse CDF of x evaluated at the probability F, and r = 0, 1, 2, ..., is a nonnegative integer. When $r = 0, \beta_0$ is equal to the mean of the distribution $\mu = E[x]$.

For any distribution the r^{th} L-moment λ_r is related to the r^{th} PWM (Hosking, 1990), through:

$$\lambda_{r+1} = \sum_{k=0}^{r} \beta_k (-1)^{r-k} \binom{r}{k} \binom{r+k}{k}$$

(1.3)

For example, the first four L-moments are related to the PWMs using:

$$\lambda_1 = \beta_0 \tag{1.4}$$

$$\lambda_2 = 2\beta_1 - \beta_0 \tag{1.5}$$

$$\lambda_3 = 6\beta_2 - 6\beta_1 + \beta_0 \tag{1.6}$$

$$\lambda_4 = 20\beta_3 - 30\beta_2 + 12\beta_1 - \beta_0 \tag{1.7}$$

Hosking (1990) defined L-moment ratios as:

L-coefficient of variation, L-CV
$$(\tau_2) = \lambda_2 / \lambda_1$$
 (1.8)

L-coefficient of skewness, L-skew
$$(\tau_3) = \lambda_3 / \lambda_2$$
 (1.9)

L-coefficient of kurtosis, L-kurtosis (
$$\tau_4$$
) = λ_4 / λ_2 (1.10)

Screening of Data Using Discordancy Measure Test

The objective of screening of data is to check that the data are appropriate for performing the regional flood frequency analysis. In this study, screening of the data was performed using the L-moments based Discordancy measure (D_i). Hosking and Wallis (1997) defined the

$$\overline{u} = N^{-1} \sum_{i=1}^{N} u_{i} \tag{1.11}$$

National Institute of Hydrology, Roorkee

Discordancy

measure (D_i) considering if there are N sites in the group. Let $u_i = [t_2^{(i)} \ t_3^{(i)} \ t_4^{(i)}]^T$ be a vector

$$A_{m} = \sum_{i=1}^{N} (u_{i} - \overline{u})(u_{i} - \overline{u})^{T}$$
 (1.12)

containing the sample L-moment ratios t_2 , t_3 and t_4 values for site i, analogous to their regional values termed as τ_2 , τ_3 , and τ_4 , expressed in Eqs. (1.8) to (1.10). T denotes transposition of a vector or matrix. Let be the (unweighted) group average. The matrix of sums of squares and cross products is defined as:

The Discordancy measure for site i is defined as:

$$D_{i} = \frac{1}{3} N (u_{i} - \overline{u})^{T} A_{m}^{-1} (u_{i} - \overline{u})$$
 (1.13)

The site i is declared to be discordant, if D_i is greater than the critical value of the Discordancy statistic D_i , given in a tabular form by Hosking and Wallis (1997).

Test of Regional Homogeneity

For testing regional homogeneity, a test statistic H, termed as heterogeneity measure was proposed by Hosking and Wallis (1993). It compares the inter-site variations in sample L-moments for the group of sites with what would be expected of a homogeneous region. The inter-site variation of L-moment ratio is measured as the standard deviation (V) of the at-site L-CV's weighted proportionally to the record length at each site. To establish what would be expected of a homogeneous region, simulations are used. A number of, say 500, data regions are generated based on the regional weighted average statistics using a four parameter distribution e.g. Kappa distribution. The inter-site variation of each generated region is computed and the mean (μ_v) and standard deviation (σ_v) of the computed inter-site variation is obtained. Then, heterogeneity measure H is computed as:

$$H = \frac{V - \mu_{V}}{\sigma_{V}} \tag{1.14}$$

The criteria for assessing heterogeneity of a region are: if H < 1, the region is acceptably homogeneous; if $1 \le H < 2$, the region is possibly heterogeneous; and if $H \ge 2$, the region is

Identification of Robust Regional Frequency Distribution

The choice of an appropriate frequency distribution for a homogeneous region is made by comparing the moments of the distributions to the average moments statistics from regional data. The best fit distribution is determined by how well the L-skewness and L-kurtosis of the fitted distribution match the regional average L-skewness and L-kurtosis of the observed data (Hosking and Wallis, 1997). The goodness-of-fit measure for a distribution, Z_i^{dist} – statistic defined by Hosking and Wallis (1997) is expressed as:

$$Z_i^{\text{dist}} = \frac{\left(\frac{-R}{\tau_i} - \tau_i^{\text{dist}}\right)}{\sigma_i^{\text{dist}}}$$
(1.15)

Where, τ_i^{-R} is weighted regional average of L-moment statistic i, τ_i^{dist} and σ_i^{dist} are the simulated regional average and standard deviation of L-moment statistics i, respectively, for a given distribution. The fit is considered to be adequate if $|Z_i^{dist}|$ -statistic is sufficiently close to zero, a reasonable criterion being $|Z_i^{dist}|$ -statistic less than 1.64.

Study Area and Data Availability

Mahanadi Subzone 3(d) in India comprises of Mahanadi, Brahmani and Baitarani basins. It is located between longitudes of 80° 25' to 87° east and latitudes 19° 15' to 23° 35' north (Fig. 3). Its total drainage area is about 1,95, 256 km². About 50% of the area of this Subzone is hilly varying from 300 m to 1350 m. Rest of the area lies in the elevation range of 0 to 300 m. The normal rainfall over the region varies from 1200 to 1600 mm. The Subzone receives about 75% to 80% of the annual rainfall from South-West monsoon during the monsoon season from June to September. The red and yellow soils cover major part of the Subzone. The red sandy, submontane and coastal alluvial soils cover the remaining part of the Subzone. The Subzone has an extensive area under forest. Paddy is the main crop grown on the cultivable land. Annual maximum peak flood data of 23 Bridge sites lying in the hydrometeorologically homogeneous region (Central Water Commission, 1982) of Mahanadi Subzone 3 (d) as well as the catchment areas of the Bridge sites were available for the study.

Analysis and Discussion of Results

Regional flood frequency analysis was performed using the various frequency distributions: viz. Extreme value (EV1), Generalized extreme value (GEV), Logistic (LOS), Generalized logistic (GLO), Normal (NOR), Generalized normal (GNO), Uniform (UNF), Pearson Type-III (PE3), Exponential (EXP), Generalized Pareto (GPA), Kappa (KAP), and five parameter Wakeby (WAK). Screening of the data, testing of regional homogeneity, identification of the regional distribution and development of regional flood frequency relationships are described below.

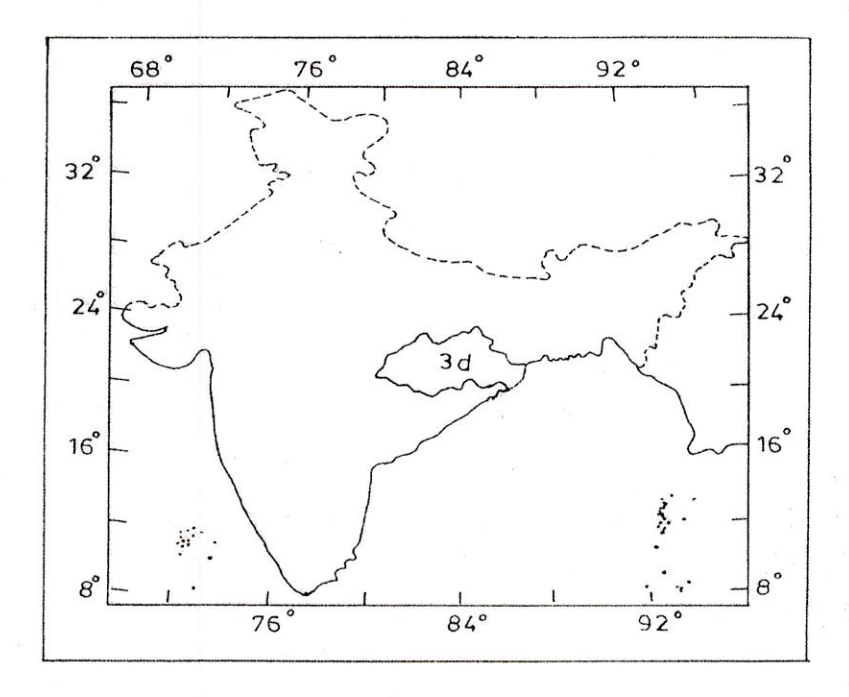


Fig. 3. Index map showing location of Mahanadi Subzone 3(d) in India

Screening of Data Using Discordancy Measure Test

Values of Discordancy statistic have been computed in terms of the L-moments for all the 23 gauging sites of the study area. It is observed that the D_i values (Hosking and Wallis, 1997) for all the 23 sites vary from 0.04 to 3.06. As 3.06 is greater than the critical value of D_i i.e. 3.00 for a region defined by 15 or more sites; hence, the site having D_i value of 3.06 is discarded from the analysis. The D_i values for 22 sites vary from 0.04 to 2.32 and the data of 22 sites may be considered suitable for regional flood frequency analysis.

Test of Regional Homogeneity

The value of the heterogeneity measure (H) was computed for the study area by carrying out 500 simulations using the Kappa distribution utilising the data of 22 gauging sites. Using the data of 22 sites, (H1), (H2) and (H3) values are computed as 4.21, 1.79 and 0.16, respectively. As these values are greater than 1.00 and even 2.0; hence, D_i is computed by discarding the sites having higher values of D_i. The data sample comprising of 15 gauging sites and yielding (H1), (H2) and (H3) values as 1.68, -0.71 and -1.98 is considered as homogeneous. The details of catchment data and statistical parameters including the discordancy measure, for the 15 gauging sites are given in **Table 2**. The values of heterogeneity measures computed by carrying out 500 simulations using the Kappa distribution based on the data of 15 sites are given in **Table 3**.

Table 2. Catchment area, sample statistics, sample size and discordancy measure for 15 gauging sites of Mahanadi Subzone 3(d)

Stream Gauging Site	Catchment Area (km²)	Mean Annual Peak Flood (m³/s)	Sample Size (Years)	L-CV (τ ₂)	L-skew (τ ₃)	L- kurtosis (τ4)	Discordancy Measure (D _i)
48	109	103.90	30	0.4020	0.2950	0.1658	0.46
93 K	. 74	153.07	28	0.2740	0.1235	0.1974	1.44
59 KGP	30	72.89	29	0.4079	0.2770	0.1780	0.74
308	19	41.22	27	0.3461	0.2339	0.0882	0.87
332NGP	225	188.59	22	0.2899	0.2117	0.2020	1.23
59 BSP	136	196.23	22	0.4068	0.3471	0.2283	1.48
698	113	247.00	25	0.4240	0.3210	0.1356	1.09
121	1150	1003.86	21	0.2690	0.1622	0.0787	1.19
332KGP	175	71.83	24	0.3102	0.1569	0.1647	0.51
40 K	115	260.67	21	0.3469	0.2328	0.1784	0.14
42	49	53.50	20	0.2260	0.0488	0.0530	1.92
69	173	238.89	19	0.3457	0.2392	0.1455	0.08
90	190	130.73	11	0.3570	0.1566	0.1335	2.11
195	615	963.77	13	0.2394	0.1305	0.1614	1.10
235	312	176.14	14	0.3128	0.2205	0.1130	0.63

Table 3. Heterogeneity measures for 15 gauging sites of Mahanadi Subzone 3(d)

Heterogeneity measures	Values
Standardized test value H	1.68
Standardized test value H(2)	-0.71
Standardized test value H(3)	-1.98

Identification of Robust Regional Frequency Distribution

The L-moment ratio diagram and $|Z_i^{dist}|$ –statistic are used as the best fit criteria for identifying the robust distribution for the study area. The regional average values of L-skewness i.e. τ_3 = 0.2180 and L-kurtosis i.e. τ_4 = 0.1510 are obtained. Figure 4 shows the L-moments ratio diagram for the study area. The Z_i^{dist} –statistic for various three parameter distributions is given in Table 4. It is observed that the $|Z_i^{dist}|$ –statistic values are lower than 1.64 for the three distributions viz. GEV, GNO and PE3. Further, the $|Z_i^{dist}|$ –statistic is found to be the lowest for GNO distribution i.e. 0.22. Thus, based on the L-moment ratio diagram and $|Z_i^{dist}|$ –statistic criteria, the GNO distribution is identified as the robust distribution for the study area. The values of regional parameters for the various distributions which have Z^{dist} –statistic value less than 1.64 as well as the five parameter Wakeby distribution are given in Table 5.

The regional parameters of the Wakeby distribution have been included in Table 5 because, the Wakeby distribution has five parameters, more than most of the common distributions and it can attain a wider range of distributional shapes than can the common distributions. This makes the Wakeby distribution particularly useful for simulating artificial data for use in studying the robustness, under changes in distributional form of methods of data analysis. It is preferred to use Wakeby distribution for heterogeneous regions.

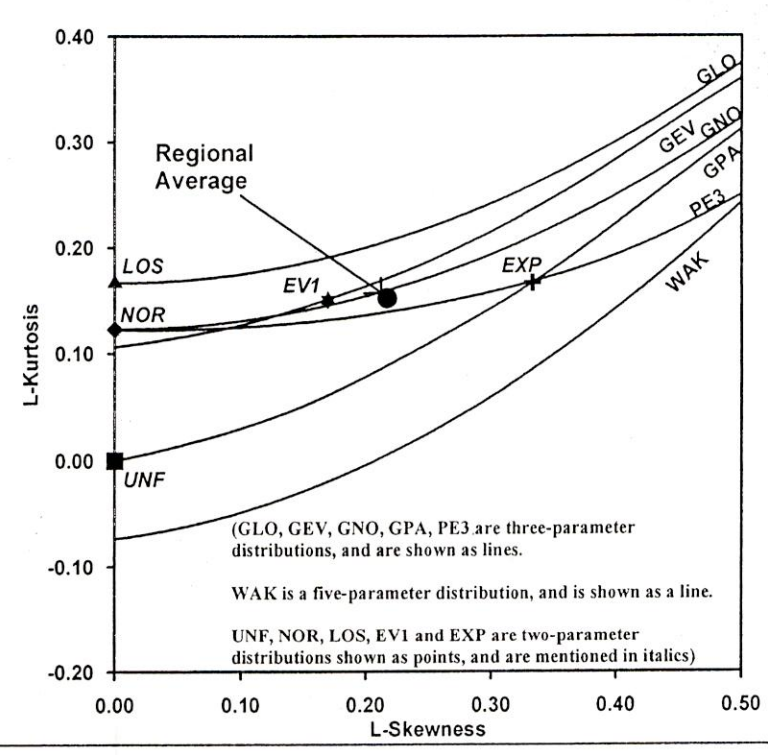


Fig. 4. L-moment ratio diagram for Mahanadi Subzone 3(d) for various distributions

Table 4: Zi dist statistic for various distributions for Mahanadi Subzone 3 (d)

S. No.	Distribution	Zi dist –statistic
1	Generalized logistic (GLO)	2.08
2	Generalized Extreme Value (GEV)	0.66
3	Generalized Normal (GNO)	0.22
4	Pearson Type III (PE3)	-0.62
5	Generalized Pareto (GPA)	-2.68

Table 5. Regional parameters for various distributions for Mahanadi Subzone 3 (d)

Distribution		Parameters of the Distribution								
GNO	$\xi = 0.870$	$\alpha = 0.548$	k = -0.451							
PE3	$\mu = 1.000$	$\sigma = 0.629$	$\gamma = 1.316$							
GEV	$\xi = 0.704$	$\alpha = 0.452$	K = -0.073							
WAK	$\xi = 0.100$	$\alpha = 1.985$	$\beta = 6.486$	$\gamma = 0.684$	$\delta = -0.078$					

Regional Flood Frequency Relationship for Gauged Catchments

For estimation of floods of various return periods for gauged catchments regional flood frequency relationship has been developed based on the robust identified GNO distribution. The cumulative density function of the three parameter GNO distribution as parameterized by Hosking and Wallis (1997) is given below.

$$F(x) = \phi(-k^{-1}\log\{1 - k(x - \xi)/\alpha\})$$
 (1.16)

Where, ξ , α and k are its location, scale and shape parameters, respectively. When, k = 0, it becomes normal distribution with parameters ξ and α . This distribution has no explicit analytical inverse form.

Floods of various return periods may be computed by multiplying mean annual peak flood of a catchment by the corresponding values of growth factors of GNO distribution given in **Table 6**.

Table 6: Values of growth factors (Q_T/\overline{Q}) for Mahanadi Subzone 3 (d)

Distri-	Return period (Years)										
bution	2	10	25	50	100	200	1000				
	Growth factors										
GNO	0.870	1.821	2.331	2.723	3.125	3.538	4.552				
PE3	0.866	1.842	2.329	2.683	3.028	3.366	4.134				
GEV	0.872	1.809	2.332	2.745	3.175	3.627	4.767				
WAK	0.865	1.848	2.353	2.712	3.052	3.374	4.058				

Regional Flood Frequency Relationship for Ungauged Catchments

For ungauged catchments the at-site mean cannot be computed in absence of the observed flow data. Hence, a relationship between the mean annual peak flood of gauged catchments in the region and their pertinent physiographic and climatic characteristics is needed for estimation of the mean annual peak flood. **Figure 5** shows a plot of the mean annual peak flood versus.

catchment area in log domain for the 15 gauging sites of Mahanadi Subzone 3(d). The regional relationship developed for the region in log domain using least squares approach based on the data of 15 gauging sites is given below.

$$\overline{Q} = 4.483(A)^{0.736}$$
 (1.17)

Where, A is the catchment area, in km² and \overline{Q} is the mean annual peak flood in m³/s. For Eq. (1.17), the coefficient of determination is, $r^2 = 0.723$.

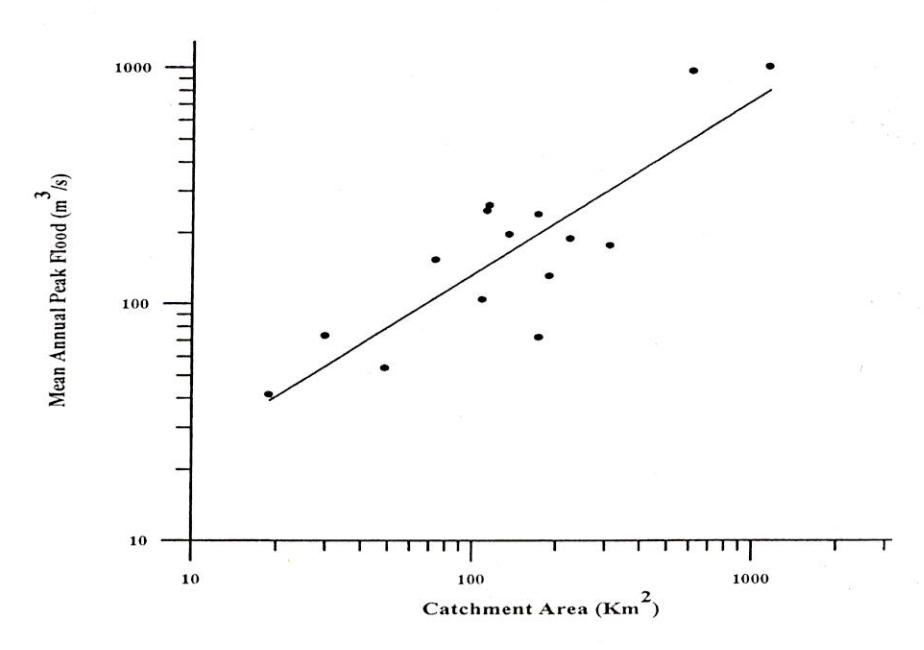


Fig. 5. Variation of mean annual peak flood with catchment area for various gauging sites of Mahanadi Subzone 3(d)

For development of regional flood frequency relationship for ungauged catchments, the regional flood frequency relationship developed for gauged catchments is coupled with regional relationship between mean annual peak flood and catchment area, given in Eq. (1.17) and following regional frequency relationship is developed.

$$Q_{\rm T} = C_{\rm T} *A^{0.736} \tag{1.18}$$

Where, Q_T is flood estimate in m^3/s for T year return period, and A is catchment area in km^2 and C_T is a regional coefficient. Values of C_T for some of the commonly used return periods are given in Table 7.

Table 7. Values of regional coefficient C_T for Mahanadi Subzone 3(d)

Distri-		Return period (Years)									
bution	2	10	25	50	100	200	1000				
2	Growth factors										
GNO	3.900	8.164	10.450	12.207	14.009	15.861	20.407				

The above regional flood formula (Eq. 1.18) may be used for estimation of floods of desired return periods for ungauged catchments of the Mahanadi Subzone 3 (d).

Impact of Climate Change on Floods of Various Return Periods -A Case Study

For evaluation of impact of climate change on floods of various return periods data of 98 years of a snow and rainfed dam have been used. Floods of various return periods have been estimated using the annual maximum peak flood series of 98 years of the study areas employing the L-moments approach.

Scenario-1:

Under Scenario-1 of climate change the highest 20% values of the annual peak flood have been increased by 20%.

Scenario-2:

Under Scenario- of climate change the highest 20% values of the annual peak flood have been increased by 20% and the lowest 20% values of the annual peak flood have been decreased by 20%.

The flood estimates for various return periods for the original series and Scenario-1 and Scenario-2 are given in **Table 8**. The percentage deviations in floods of various return periods for Scenario-1 and Scenario-2 under climate change with respect to the original annual maximum peak foods series are given in **Table 9**. Figure 6, 7 and 8 shows comparison of floods for 50, 100 and 1000 years return period floods for the original series and Scenario-1 and Scenario-2 under climate change.

Table 8. Flood of various return periods for original flood series and Scenario-1 and Scenario-2 under climate change:

Return Periods	20	25	50	100	200	500	1000	10000
Original series	8548	8978	10419	12042	13883	16715	19209	30308
Scenario 1	9950	10603	12896	15657	19000	24543	29803	56911
Scenario 2	10033	10658	12810	15319	18257	22954	27247	47818

Table 9. Percentage deviations in floods of various return periods for Scenario-1 and Scenario-2 under climate change:

Return Periods	20	25	50	100	200	500	1000	10000
Scenario 1	16	18	23	30	36	46	55	87
Scenario 2	17	18	22	27	31	37	41	57

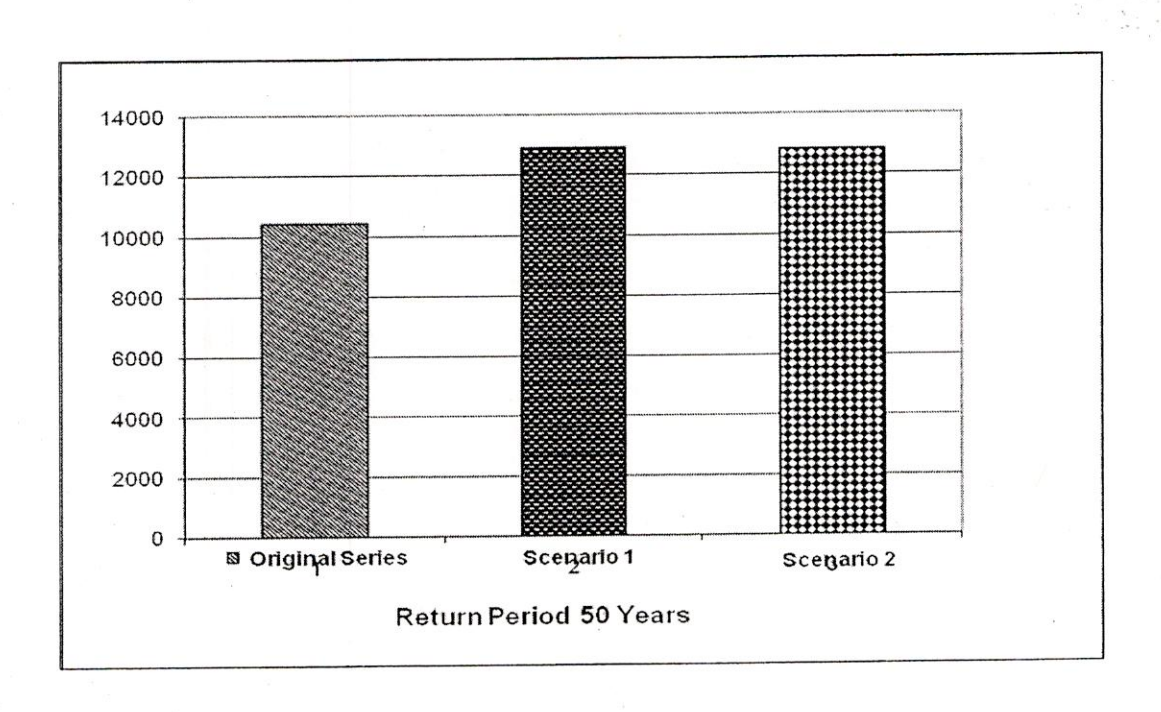


Fig. 6. Comparison of floods for 50 years return period floods for the original series and Scenario-1 and Scenario-2 under climate change

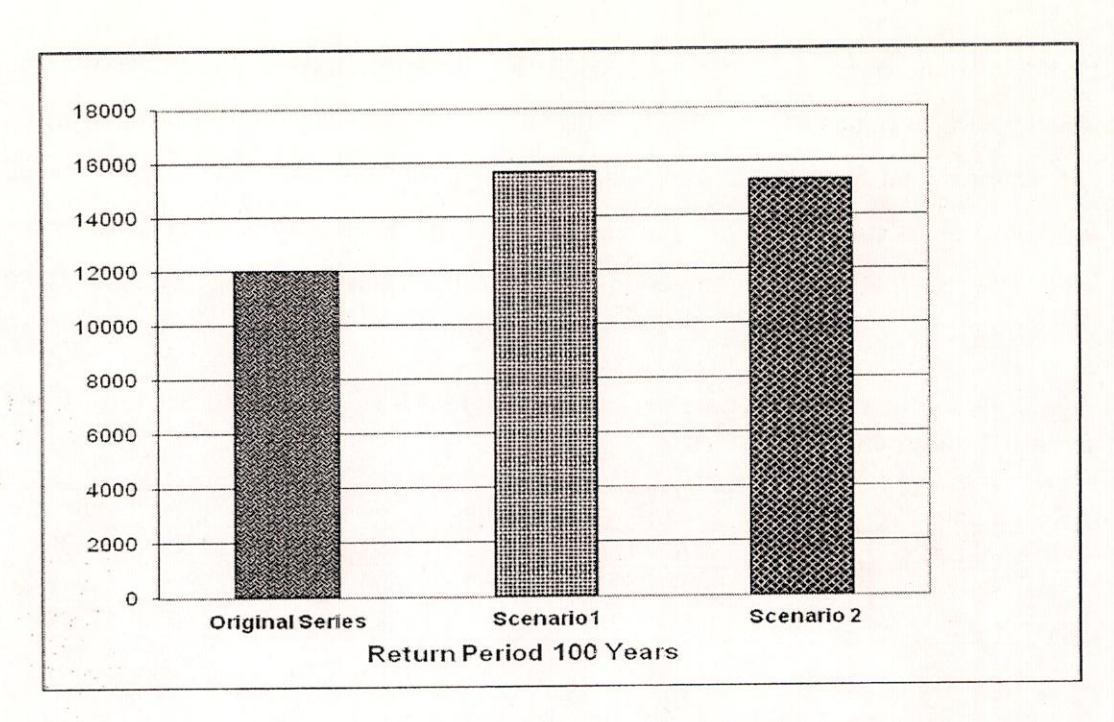


Fig. 7. Comparison of floods for 100 years return period floods for the original series and Scenario-1 and Scenario-2 under climate change

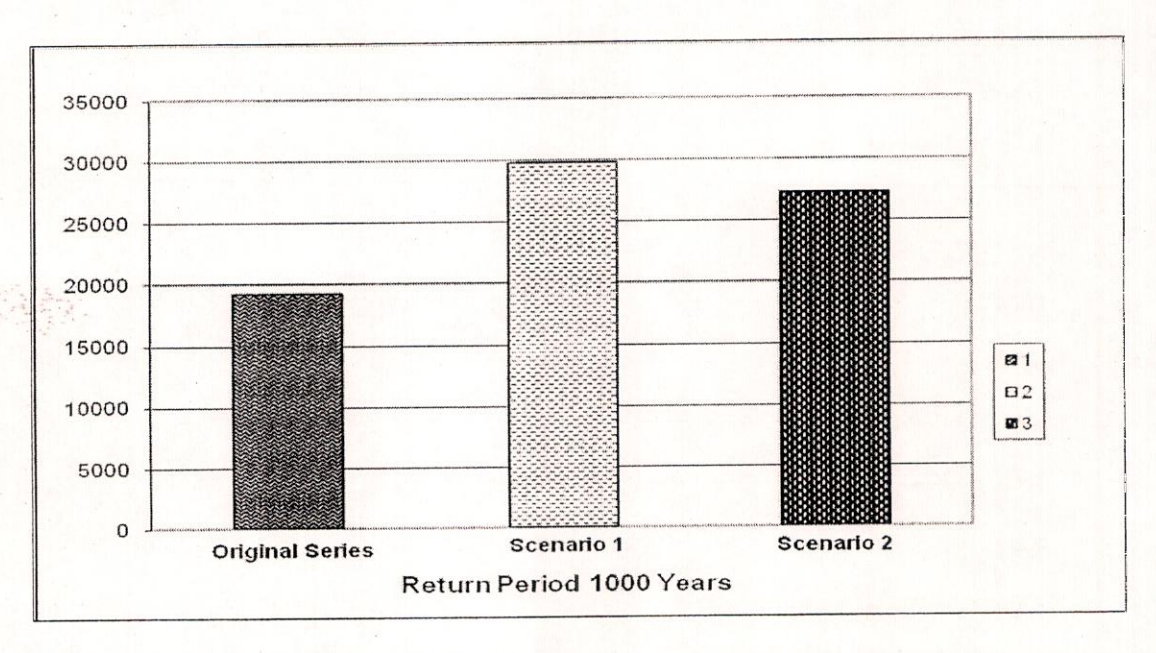


Fig. 8. Comparison of floods for 1000 years return period floods for the original series and Scenario-1 and Scenario-2 under climate change

IMPACT OF CLIMATE CHANGE ON PROBABLE MAXIMUM FLOOD – A CASE STUDY

For evaluation of impact of climate change on Probable Maximum Flood (PMF) a case study

for a snow and rainfed catchment of above 5000 km² has been carried out considering the following possible cases due to climate change.

- (a) Impact of change of sequencing of rainfall
- (b) Impact of increase in peak of the unit hydrograph
- (c) Impact of change of Temporal Distribution Pattern of Design Storm
- (d) Impact of change of loss rate

For estimation of design flood, 1-hour unit hydrograph has been derived using the Clark IUH model. The parameters of Clark IUH model have been estimated as $T_c = 9$ and R = 12. The unit hydrograph which is derived based on the principle of linearity, has been applied to convert the excess rainfall hyetograph into direct surface runoff hydrograph. The design loss rate of 1-mm/hour has been adopted for computation of design excess rainfall hyetograph from the design storm values. Based on analysis of the observed flow records, design base flow of 340 m³/s has been added with the ordinates of design direct surface runoff hydrograph for estimation of the PMF hydrographs.

(a)Impact of change of sequencing of rainfall

Due to climate change the rainfall pattern including intensity of rainfall, depth of rainfall, number of rain days are likely to be changed. Due to aforementioned changes and other factors the pattern and sequence of rainfall over short duration are likely to change. This aspect has been studied as given below. A comparison of the considered possible changes with reference to the conventional practice of design storm has also been examined.

Probable maximum flood has been estimated by converting the 2-days PMP value and its time distribution into 48 hour design storm and convoluting it with the unit hydrograph derived based on the Clark IUH model. The PMFs estimated based on the conventional critical sequencing of the 48-hours design storm approach² as well as recent approach of multiple bells design storm approach³ have been compared. As the multiple bell approach³ does not provide details of arrangement of 1-hourly excess-rainfall values within the one or two bells per day of the design storm the following four cases of storm patterns have been studied and PMF estimates resulting from these cases are compared for identifying the rational pattern of design storm for optimal design flood estimation.

- (i) Design storm as single bell (Case -1), as shown in Figure 9,
- (ii) Design storm as two bells (Case 2), as shown in Figure 10,
- (iii) Design storm as four bells (Case 3), as shown in Figure 11, and
- (iv) Design storm as four bells (Case 4), as shown in Figure 12.

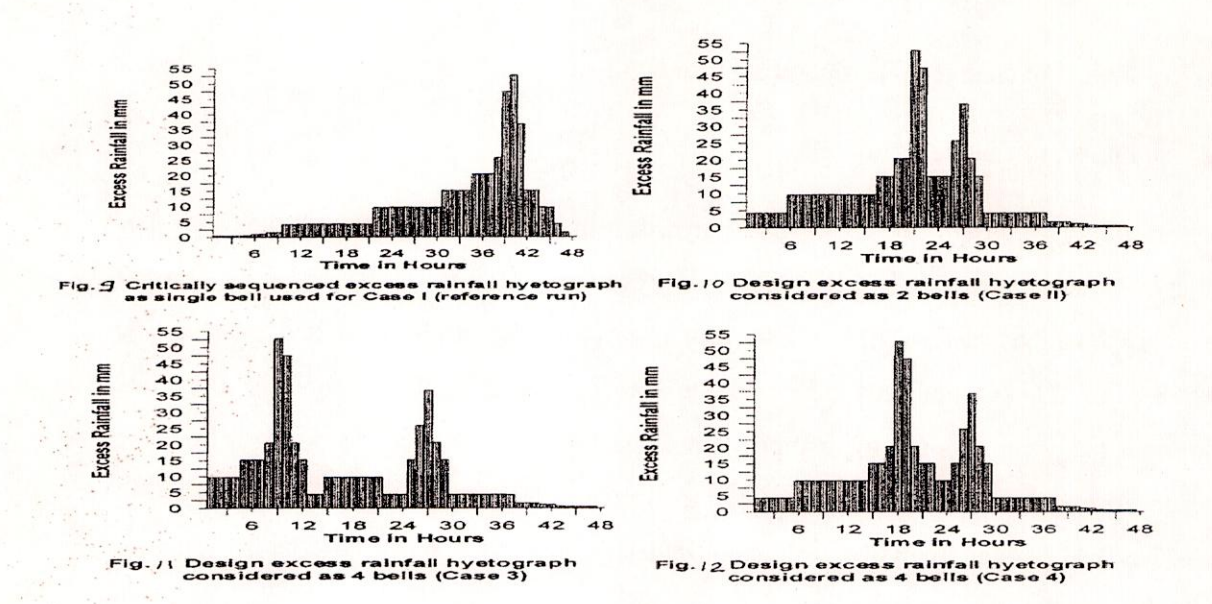


Table 10: Design flood peak (Q_p) and time to peak (T_p) and the percentage variation with respect to the values of the reference run for various storm patterns

S. No.	Design storm Patterns	Peak (Q _p) (m ³ /s)	Percent deviation in Q _p	Time to Peak (T _p) (Hours)	Percent deviation in T _p
1	1 Bell (Case – 1) (Reference run)	24359	Reference run	49	Reference run
2	2 Bells (Case – 2)	22407	-8.0	35	-28.6
3	4 Bells (Case-3)	17369	-28.7	19	-61.2
4	4 Bells (Case-4)	21121	-13.3	35	-28.6

(b) Impact of increase in peak of the unit hydrograph

To study the impact of increase in peak of the unit hydrograph on the design flood peak, different unit hydrographs have been applied with the design storm of one bell (considered to be reference design storm). Fig. 11 shows variation of percentage increase in the peak of the unit hydrograph. It may be observed from the Fig. 11 that for 50% increase in the peak of unit hydrograph there is an increase of about 25% in the design flood peak.

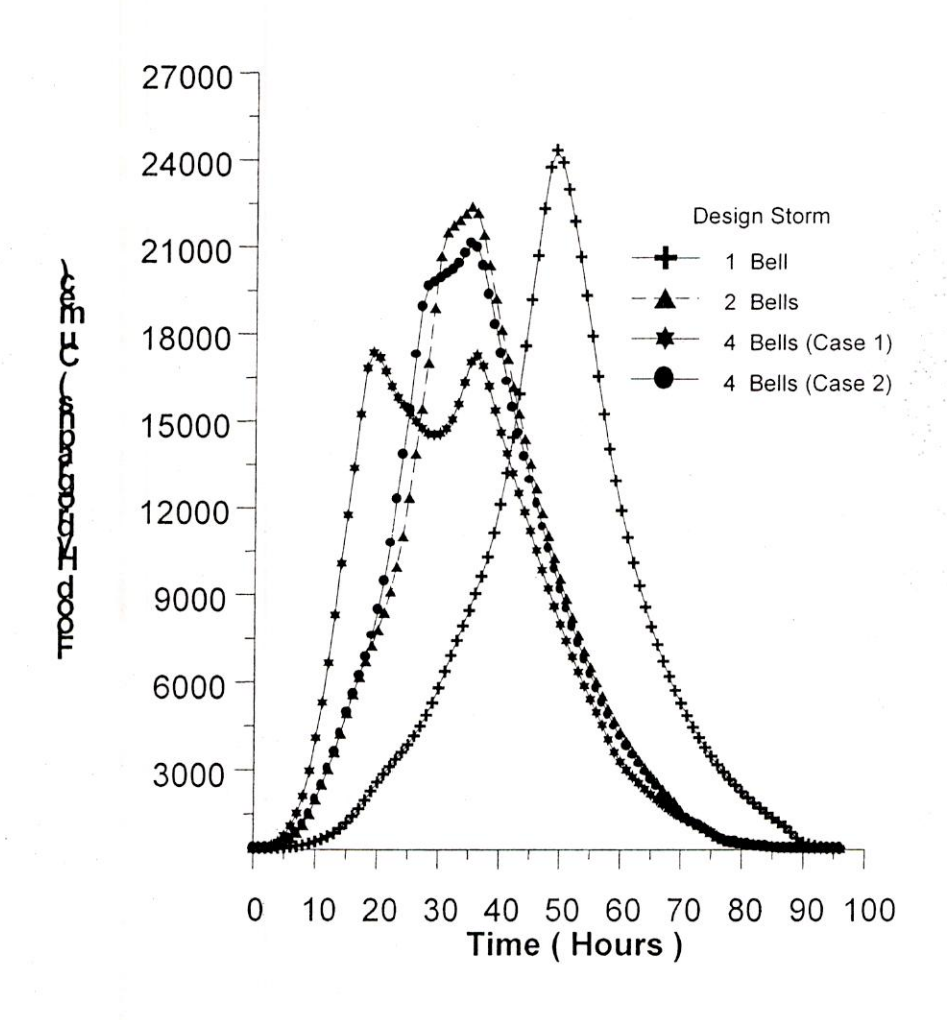


Fig. 13: Design flood hydrographs for various storm patterns

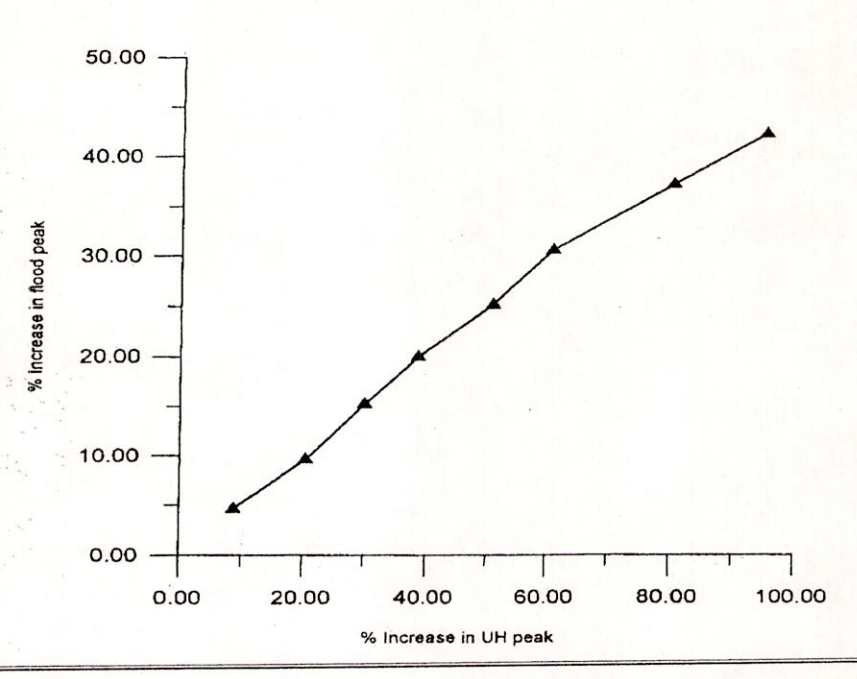


Fig.14. Variation of percentage increase in peak of flood hydrograph with percentage increase in peak of UH

The pattern of temporal distribution of design storm also plays a significant role in determining the peak of the design storm hydrograph. Whenever, the problem is referred to IMD, the IMD provides the values of the PMP along with its temporal distribution within bells to be used for design flood estimation as per the recommendations of WMO. Whenever, there is concurrent data of the storm under consideration for design the time distribution of areal rainfall over the catchment is recommended (CWC, 1993). In this study, the sensitivity of the temporal distribution of storm pattern has been conducted by considering two more distribution patterns apart from the storm pattern available for the design storm. The design storm distribution adopted for the reference run as well as the two other distribution patterns considered in the study are shown in Fig.17.

The design flood hydrographs of the design storm distributions of the reference run as well as for the two sensitivity runs are shown in Fig. 18. It is seen from the figure that the design flood peak decreases from 24,359 (reference run/distribution pattern 1) to 20,023 cumec i.e. by 17.8% for the design storm distribution pattern 2. Whereas, for the design storm pattern 3, the peak

increases to 27,745 viz. 13.9%. The time to peak does not get effected for the above cases. It shows that the design storm pattern affects the peak of the design flood hydrograph very significantly.

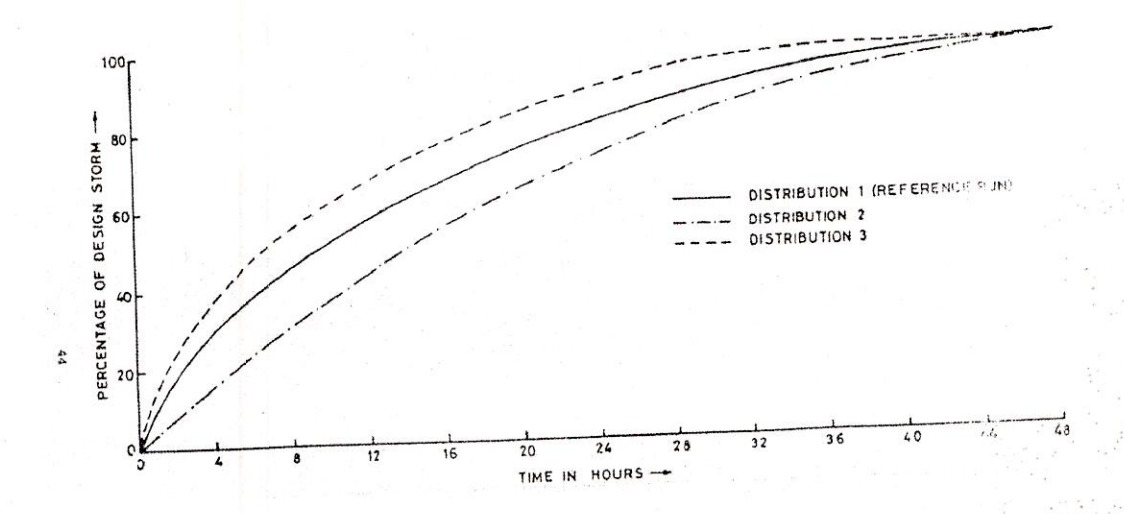


Fig. 15. Various percentage design storm distribution patterns

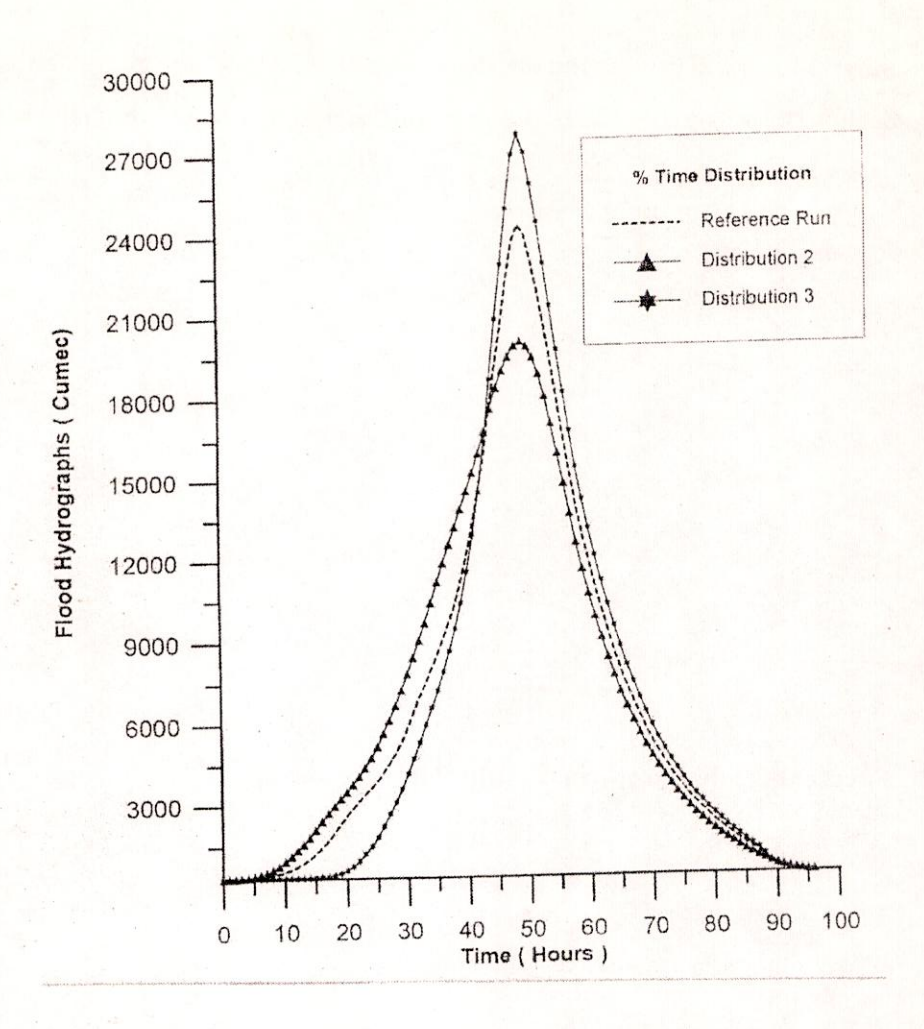


Fig.16. Design flood hydrographs for various percentage design storm distribution patterns

(d) Impact of change of Design Loss Rate

In order to study the sensitivity of the design flood peak to change in loss rate values sensitivity run have been taken up for the uniform loss rates of 0.0, 0.5, 1.0, 1.5, 2.0, 2.5, 3.0, 3.5 and 4.0 mm/hour, considering other design parameters same as for the reference run. Fig.16 shows the variation of percentage decrease in peak of the flood hydrograph with increase in loss rate. Variation of peak (Qp) and time to peak (Tp) of the design flood hydrograph with loss rate is shown in Table-4. It is seen from the Table -4 that with increase in loss rate the peak of the design flood hydrograph decreases.

The percentage decrease corresponding to loss rate of 4 mm/hour (400% increase) is only 15%, with respect to the reference run. It indicates that the design flood hydrograph is not much sensitive to the lost rate.

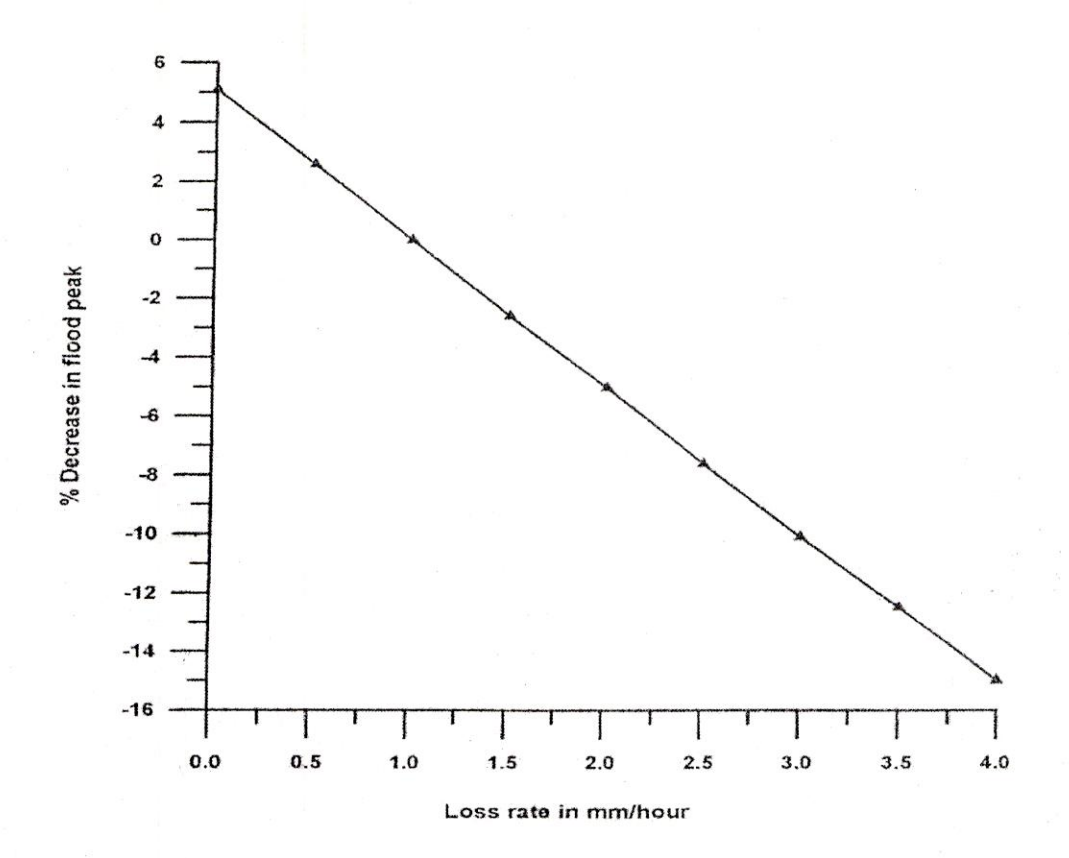


Fig. 17: Variation of percentage decrease in peak of flood hydrograph with loss rate

BIBLIOGRAPHY

A. Zafirakou-Koulouris, R.M. Vogel, S.M. Craig, and J. Habermeier, L moment diagrams for censored observations. Water Resources Research, 34(5), 1241-1249 (1998).

Central Water Commission, Flood Estimation Report for Mahanadi Subzone 3 (d) (Directorate of Hydrology (Small Catchments), New Delhi, 1982).

D.H. Pilgrim, and I. Cordery, *Flood runoff. In Handbook of Hydrology* (Mc Graw-Hill, Inc, New York, 1992).

IPCC 2001. Climate Change 2001: The Scientific Basis, Contribution of Working Group I to the Third Assessment Report of the Intergovernmental Panel on Climate Change-2001 (eds. J.T. Houghton et al.), Published for the Intergovernmental Panel on Climate Change by Cambridge University Press.

IPCC 2007. Climate Change 2007: Final report on climate change by Intergovernmental Panel, Published for the Intergovernmental Panel on Climate Change, Cambridge University Press.

J.A. Greenwood, J.M. Landwehr, N.C. Matalas, and J.R. Wallis, Probability weighted moments: Definition and relation to parameters of several distributions expressible in inverse form. Water Resources Research, 15(5), 1049-1054 (1979).

J.R. Stedinger, R.M. Vogel, and E. Foufoula-Georgiou, *Frequency analysis of extreme events, In Handbook of Hydrology* (ed. D.R. Maidment, Chap.18, McGraw-Hill Inc., New York, 1992).

J.R.M. Hosking, and J.R. Wallis, *Regional frequency analysis-an approach based on L-moments* (Cambridge University Press, New York, 1997).

J.R.M. Hosking, and J.R. Wallis, Some statistics useful in regional frequency analysis. Water Resources Research, 29(2), 271-281 (1993).

J.R.M. Hosking, L-moments: Analysis and estimation of distributions using linear combinations of order statistic. J. Royal Stat. Soc., Series B, 52(2), 105-124 (1990).

K. Chokmani, and T.B.M.J. Quarda, Physiographical space-based kriging for regional flood frequency estimation at ungauged sites. Water Resources Research, 40, W12514, doi:10.1029/2003WR002983 (2004).

Kaczmarek, Z.D. Jurak and J.J. Napioekowski, Impact of climate change on water resources in Poland. Publication of Institute of Geophysics, Polish Academy of Science, E-1(295), 51 p, 1997

Karl, T.R., Some spatial characteristics of drought duration in the United States. Journal of Climate and Applied Meteorology, 22(8), 1356-1366, 1983.

Kundzewicz, Z.W. and Zdislaw Kaczmarek, Copping with hydrological extremes. Jour. of Water International. International Water Resources Association, 15(1), 66-75, 2000

Pandey, R.P. and K.S. Ramasastri, 'Relationship between the common climatic parameters and average drought frequency. Hydrological Processes Journal, 15(6), pp. 1019-1032, 2001.

Pandey, R.P., S.K. Mishra, K.S Ramasastri, Ranvir Singh and V.P. Singh, Drought tendencies in north-western region of India. International conference on Water Resources Management in arid regions, March 23-27, 2002, Kuwait, 2002.

Ponce, V.M., R.P.Pandey and Sezan Ercan, 'Characterization of drought across climatic spectrum'. Journal of Hydrologic Engineering, ASCE, 5(2), pp 222-224, 2000.

R. Kumar, and C. Chatterjee, Regional flood frequency analysis using L-moments for North Brahmaputra Region of India. J. Hydrologic Engineering, ASCE, 10(1), 1-7 (2005).

R. Merz, and G. Bloschl, Flood frequency regionalization – spatial proximity vs. catchment attributes. Journal of Hydrology, 302, 283-306 (2005).

R.M. Vogel and N.M. Fennessey, L-moments should replace product moments diagrams. Water Resources Research, 29(6), 1745-1752 (1993).

V. Iacobellis and M. Fiorentino, Derived distribution of floods based on the concept of partial area coverage with a climatic appeal. Water Resources Research, 36(2), 469-482 (2000).

Wilhite Donalt A. Drought as a natural Hazard: concept and definition. In drought: A Global assessment, Natural Hazards and Disaster Series, Vol. 1, Wilhite Donalt A (eds), Routledge Publisher, UK, Chapter 1, 2000.

Z. Jingyl, and M.J. Hall, Regional flood frequency analysis for the Gan-Ming river basin in China. Journal of Hydrology, 296, 98-117 (2004).

*** **** ***